ACS APPLIED MATERIALS & INTERFACES

Research Article

www.acsami.org

A Calcium Phosphate Nanoparticle-Based Biocarrier for Efficient Cellular Delivery of Antisense Oligodeoxynucleotides

Shenglei Hou,[†] Hongmei Ma,[†] Yuxuan Ji, Wenyue Hou, and Nengqin Jia*

The Education Ministry Key Laboratory of Resource Chemistry, Department of Chemistry, Life and Environmental Science College, Shanghai Normal University, Shanghai 200234, China

ABSTRACT: Antisense oligodeoxynucleotides (ASODNs) can bind to some specific RNA of survivin can prevent the mRNA translation at the genetic level, which will inhibit survivin expression and make the cancer cells apoptosis. However, the ASODNs-based therapies are hampered by their instability to cellular nuclease and their weak intracellular penetration. Here we reported a calcium phosphate (CP)-based carrier to achieve efficient delivery of ASODNs into cells. In this study, we used a facile microemulsion approach to prepare spherical and porous ASODNs-CP nanoparticles (ASODNS-CPNPs) with the size of 50-70 nm in diameter, and their structure, morphology and composition were characterized by TEM, XRD, FTIR, ICP and DLS, UV-Vis spectroscopy and agarose gel electrophoresis. The results indicated that the nanoparticles have a high ASODNs loading capacity. Furthermore, cellular uptake and delivery efficiency of the ASODNS-CPNPs, as well as cellular apoptosis induced by the ASODNs doping into the calcium phosphate nanoparticles, were investigated by confocal laser scanning microscopy, biological TEM, flow cytometry, and MTT assay. Efficient intracellular delivery of the nanoparticles was observed. All these results suggested that the prepared calcium phosphate nanoparticles could be used as a promising biocarrier for delivery of ASODNs.

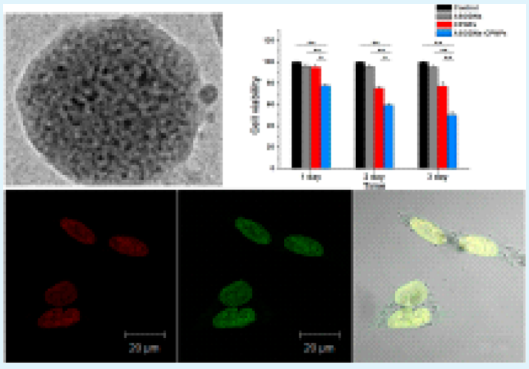

KEYWORDS: *facile microemulsion approach, loading capacity, cellular delivery, biocarrier*

INTRODUCTION

Development of technologies that promise to improve the existing methods of cancer detection and treatment is a significant challenge. Tumor-targeted delivery has emerged as one of the focused areas in cancer gene therapy. Survivin is a nuclear shuttling protein that is regarded as inhibitor of apoptosis and regulator of the cell cycle.[1] It is highly expressed during fetal development, and in precancerous and cancerous lesions, while not usually being detected in normal adult tissues,[2,3] which makes survivin a useful prognostic marker of cancer and appealing molecular target for anticancer therapeutics.[4,5] Antisense technique, a new tool in drug design, has become an emerging area of research in cancer-associated treatment during the past decades. This technology involves blocking or significantly inhibiting excessive production of a particular protein at the RNA level as a means of regulating gene expression. During this process, antisense molecule functioned as a molecular scalpel. Recently, one of the antisense molecules, antisense oligodeoxynucleotides (ASODNs), was widely used in antisense technology.[6−8] Compared with conventional drugs, ASODNs offers several advantages, such as high target specificity (segments of ASODNs are complementary to specific RNA targets), easy design, diversified multiplicity, simple synthetic and a high degree of localised and pertinence.[9] Hence, ASODNs has becomes a promising potential targeted anticancer agent in malignant tumor and cancer therapy. However, the ASODN-based therapy is hampered by the instability of ASODNs to cellular nuclease and their weak intracellular penetration. Therefore, development of effective strategies for efficient delivery of ASODNs to targeted cells is urgent needed. Many potential delivery systems have been extensively studied such as liposomes, organic polymers, and inorganic nanoparticles.[10−14] Specifically, inorganic nanoparticles (including gold nanoparticles, silica nanoparticles, and carbon nanotubes) has already exhibited its diversity and acted as promising vehicles for gene delivery in recent years.[15−22]

It is well-known that calcium phosphate coprecipitation is one of the most common in vitro approaches for transferring the helical phosphate DNA into cell lines.[23−25] Furthermore, because of its good biocompatibility, biodegradability, lack of toxicity, and stable chemical properties, calcium phosphate nanoparticles (CPNPs) could be exploited as a promising vector to deliver a broad range of therapeutics, such as proteins, antibodies, oligonucleotides and imaging agents, in a variety of biological systems.[26−29] In this work, we used the double reverse emulsion approach to prepare CPNPs as ASODNs delivery vehicle and achieved high cellular transfection efficiency. ASODNs could be directly incorporated into crystalline calcium phosphate matrices through the addition

Received: November 29, 2012
Accepted: January 11, 2013
Published: January 16, 2013

of ASODNs biomolecules to inner water phase of the W/O/W emulsion. The results demonstrated effective intracellular delivery and targeting anticancer activity in vitro of the CPNPs.

EXPERIMENTAL SECTION

Materials. The ASODNs (CCCAGCCTTCCAGCTCCTTG) and the fluorescein dye (FAM) labeling ASODNs (6′-FAM-ASODNs, 6′-FAM-CCCAGCCTTCCAGCTC

C-TTG) were purchased from Sangon (Shanghai, China). The human cervical carcinoma HeLa cells were purchased from cell bank of Chinese Academy of Science, Shanghai. Cell culture media MEM was purchased from Invitrogen Corporation (USA). RNase A Solution, propidium iodide (PI) and 3-(4, 5-dimethylthiazolyl-2-yl)-2, 5-diphenyltetrazolium bromide (MTT) were purchased from Sigma–Aldrich. All other chemicals were of analytical grade.

Preparation of ASODNs-CPNPs. The double reverse emulsion approach was used to synthesize the ASODNs-doped CPNPs. Typically, nanoparticles were synthesized by water-in-oil (W/O) microemulsion system using cyclohexane as the oil phase, the nonionic surfactant ethylene glycol monobutyl ether and the aqueous solutions of $CaCl_2$ and equimolar amount of sodium dihydrogen phosphate and sodium hydrogen phosphate as the water phase. The procedures were as follows:

(1) The aqueous solutions of 50 μL of 120 μg/mL ASODNs or 6′-FAM-ASODNs and 650 μL of 0.03 mol/L NaH_2PO_4/Na_2HPO_4 with 0.004 mol/L sodium silicate as nucleation catalyst, 4 mL of ethylene glycol monobutyl ether, and 10 mL of cyclohexane were mixed together to form Microemulsion 1. The aqueous solutions of 650 μL 0.05 mol/L $CaCl_2$, 4 mL of ethylene glycol monobutyl ether, and 10 mL of cyclohexane were mixed together to form Microemulsion 2.

(2) Microemulsion 1 and 2 were equilibrated under a constant stirring using mechanical stirrer for 5 min before they were combined to form a microemulsion mixture. After equilibrating for several minutes, 225 μL 0.001 mol/L sodium citrate as dispersing agent was added to the microemulsion mixture and react over 10 min under a constant stirring at room temperature. Then the microemulsion mixture was centrifuged at 14 000 rpm for 15 min. After centrifugation, the precipitate was successively washed with ethanol and PBS twice in order to remove the residual ethanol. Finally, the precipitate was dispersed in PBS and stored at 4°C in a refrigerator.

As control group, the aqueous solution of Microemulsion 1 without the addition of ASODNs or 6′-FAM-ASODNs was prepared to synthetize pure CPNPs, and the procedure was the same as above.

Characterization of ASODNs-CPNPs. The morphology, structure and composition of CPNPs were characterized by transmission electron microscopy (TEM), Malvern Zetasizer Nano ZS90, X-ray diffraction measurement (XRD), Fourier transform infrared spectroscopy (FTIR) and inductively coupled plasma spectrometry (ICP).

Loading Efficiency. The ASODNs-CPNPs were dispersed in 1 mL of PBS and measured by UV–vis spectrophotometry. UV-Vis absorption spectra and optical density (OD) at 260 nm were recorded by multiskan spectrum. The amount of unbound ASODNs remaining in the supernatant was calculated by the agarose gel electrophoresis and the standard curve based method.

For the agarose gel electrophoresis analysis, the microemulsion mixture was first centrifuged and unloaded ASODNs remained in the supernatant for agarose gel electrophoresis. The standard ASODNs with concentration of 6.00, 4.50, 3.00, 1.50, 0.60, and 0.45 μg/mL were prepared for agarose gel electrophoresis. The free negative ASODNs moved to the positive electrode. Next, the brightness of the supernatants and different concentrations of standard samples on the corresponding lanes of the electric field by agarose gel electrophoresis was investigated. After ethidium bromide staining, the brightness of each ASODNs band was obtained by gel electrophoresis image analysis system (Shanghai FuRi Science & Technology Co.).

The Optical density (OD) of the ASODNs at 260 nm was recorded by multiskan spectrum for the standard curve based method. The standard ASODNs were prepared with the concentrations of 0.30, 0.60, 1.20, 1.80, and 2.40 μg/mL, and the ASODNs-CPNPs were estimated by measuring the optical density of the supernatant of the pure CPNPs without ASODNs as a blank. Then the loading efficiency was determined by the equation $E\% = ((ASODNs)_o - (ASODNs)_f)/(ASODNs)_o \times 100\ \%$, where $(ASODNs)_o$ represented the optical density of the original amount of ASODNs added into the reaction mixture and $(ASODNs)_f$ represented the optical density of the nonprecipitated $(ASODNs)_f$ remaining in the supernatant.[30]

Release of ASODNs from ASODNs-CPNPs. The ASODNs were packed in the CPNPs during the synthetic process of the CPNPs. Therefore, with the dissolution of the ASODNs-CPNPs, the ASODNs could be released from ASODNs-CPNPs. The release process from ASODNs-CPNPs were monitored by detecting the remaining Ca^{2+} in the dialysate through ICP. The ASODNs-CPNPs were incubated with ultrapure water at different pH from 4 to 7 for different periods of time. Ca^{2+} released from ASODNs-CPNPs was collected by dialysis. Then, the amount of the Ca^{2+} in the dialysate was measured by ICP.

In vitro Transfection and Cellular Uptake of ASODNs-CPNPs. *Cell Culture.* HeLa cells were grown in MEM medium with 10% fetal bovine serum (FBS) and 100 mg/mL penicillin G/streptomycin in the incubator at 37 °C with 5 % CO_2 atmosphere. Before transfection experiments, cells were at a logarithmic phase and weren't detached until 90% confluence.

Flow Cytometry Analysis. Four hours after transfection, the 6′-FAM-ASODNs-CPNPs transfection medium was removed and the HeLa cells were washed several times with PBS. HeLa cells were trypsinized and then dispersed in 1 mL of PBS for flow cytometry analysis.

Confocal Laser Scanning Microscopy Analysis. To observe endocytosis of nanoparticles by the cells, the HeLa cells were incubated with the 6′-FAM-ASODNs-CPNPs in transfection medium for 4 h, and then the cells were washed several times with PBS and analyzed by the confocal laser scanning microscopy (CLSM).

In order to further discern the subcellular distribution of the ASODNs-CPNPs in the HeLa cells, the cells were co-incubated with the 6′-FAM-ASODNs-CPNPs (green color) and staining solution (containing propidium iodide, PI, red color) in culture dish, and then washed three times with PBS. The pre-made ice-cold staining solution contains 5 μg/mL propidium iodide (PI), 0.10 mg/mL RNaseA Solution, 0.5 % Triton X-100 and PBS.

Biological Transmission Electron Microscopy (TEM) Observation. HeLa cells were incubated with the ASODNs-CPNPs for 4 h, then trypsinized, immobilized, and embedded to prepare cell section for Biological TEM.

Cell Viability Assay. HeLa cells were seeded in a 96 well cell culture plate at a density of 1×10^4 cells per well in 5% CO_2 at 37 °C for 24 h . Then, free ASODNs, CPNPs and, ASODNs-CPNPs were added to the medium, and the cells were incubated in 5% CO_2 at 37 °C for further 24 h, 48 h, and 72 h. Then the medium containing free ASODNs, CPNPs and, ASODNs-CPNPs was removed and 200 μL of MTT solution (diluted in a culture medium with a final concentration of 1 mg/mL) was added and incubated for another 4 h. The medium was then replaced with 200 μL of dimethyl sulfoxide (DMSO), and the absorbance was monitored using a microplate reader at a wavelength of 570 nm. Cytotoxicity was expressed as the percentage of cell viability compared to the untreated control cells.

RESULTS AND DISCUSSION

Characterizations of the ASODNs-CPNPs. ASODNs-CPNPs were directly synthesized by the double reverse emulsion approach. The microemulsion route was based on chemical coprecipitation that was also derived from chemical bonding between calcium ion and phosphate, which was also the backbone of ASODNs. The CPNPs can interact with ASODNs through ionic bonds to form ASODNs-CP nanocomposites. The size of this nanocomposite could be controlled

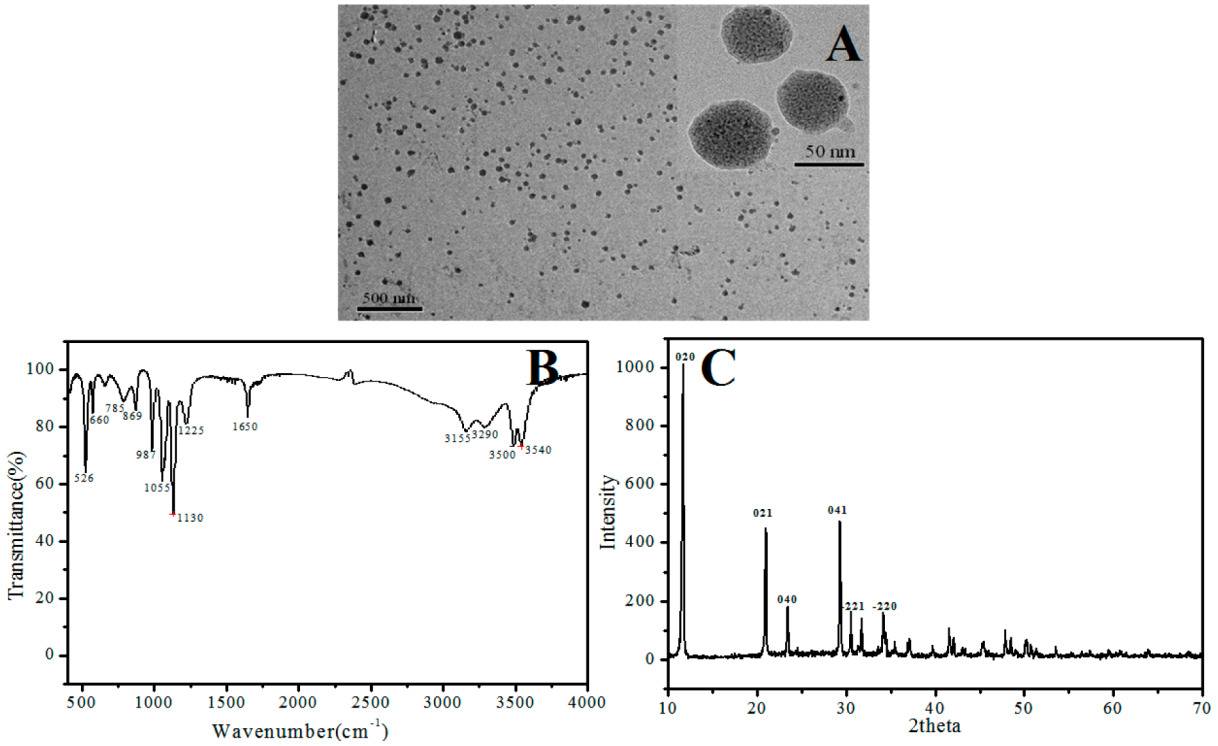

Figure 1. Characterization of ASODNs-CPNPs. (A) Transmission electron micrograph (TEM) of ASODNs-CPNPs. (Inset) enlarged part. (B) FTIR spectrum and (C) X-ray diffraction patterns (XRD) data of ASODNs-CPNPs.

by the volume ratio of aqueous solution and cyclohexane under suitable stirring condition.

Morphologic analysis of the ASODNs-CPNPs by transmission electron microscopy clearly showed that the as–prepared nanoparticles are regularly void spherical nanoparticles and the average particle size is in the range of 50-70 nm (Figure 1A). The average hydrodynamic diameter of ASODNs-CPNPs was about 68 nm with a narrow particle size distribution, which was consistent with TEM. The surface potential of nanoparticles was −18.6 mV as evidenced by the zeta potential of laser Doppler electrophoresis. The negative potential might result from citrate ions which were on the surface of nanoparticles.

As shown in Figure 1B, the XRD pattern gave a series of diffraction broad peaks assigned mainly to brushite phase. The peak around 11.7, 21.0, 23.5, 29.3, 30.5, and 34.2° corresponding to Miller indices of (020), (021), (040), (041), (−221), (−220) are observed in the diffractograms of nanoparticles. The peak at 31.7° (021) corresponds to the presence of hydroxyapatite and the wide and small diffraction peaks indicate the low degree of crystallinity and small crystal size.[31] In addition, the prepared nanoparticles were characterized by the FTIR spectra (Figure 1C). The characteristic absorbance peaks at 577 and 526 cm^{-1}, 1130 and 1055 cm^{-1}, and 987 cm^{-1} correspond to PO_3^{4-} or HPO_3^{4-} group. The absorption peaks at 3540, 3500, and 660 cm^{-1} corresponds to the flexural and stretching vibrations of the lattice OH^- ions respectively. The absorption peaks at 3290, 3155, and 1650 cm^{-1} are due to the crystallized water. In addition, the FTIR absorption of citrate was also used to confirm existence of citrate on the surface of the nanoparticles. The characteristic peaks of citrate at 1225, 869, and 785 cm^{-1} corresponds to CO_3^{2-} group vibration, which is attributed to sodium citrate used during the preparation. Therefore, the FTIR spectra and XRD measurements indicated the formation of low crystallized hydroxyapatite at the early stages of precipitation, which has either been converted to crystallized hydroxyapatite or got dissolved.[32]

The calcium and phosphate ratio was measured by ICP. The molar ratio of Ca:P is 1.30:1 which is low compared to the synthesis ratio (1.67:1, corresponding to the ratio found in hydroxyapatite). It may be due to two primary factors, one is the formation of low crystallized brushite (molar ratio of Ca:P is 1:1) along with hydroxyapatite, and the other is likely due to the formation of ASODNs-CPNPs which are excluded from the particles during the synthesis.[33]

Loading Efficiency of the ASODNs-CPNPs. UV–vis absorption spectra were used to examine whether ASODNs had been loaded into the CPNPs. As shown in Figure 2, the ASODNs-CPNPs have two absorption peaks which appear at

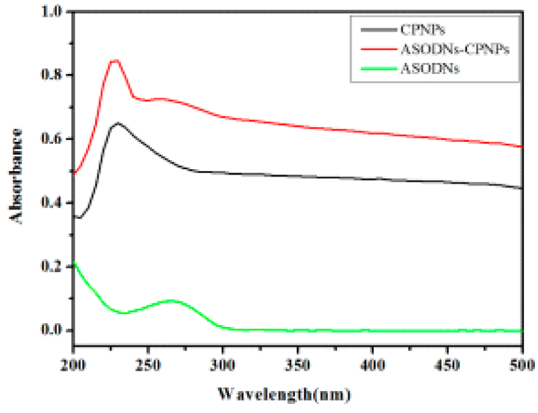

Figure 2. UV–vis absorption spectra of the ASODNs-CPNPs (red), ASODNs (green), and CPNPs (black) obtained in PBS.

dx.doi.org/10.1021/am3028926 | ACS Appl. Mater. Interfaces 2013, 5, 1131–1136

the wavelength of 230 and 260 nm. In contrast, the UV−vis absorption peak of free ASODNs and pure CPNPs was observed at 260 and 230 nm, respectively. It indicated that the ASODNs are successfully loaded into the CPNPs.

As shown in Figure 3A, it can be seen the brightness of the standard ASODNs prepared with concentrations of 6.00, 4.50, 3.00, 1.50, 0.60, and 0.45 μg/mL (from Lane 1 to Lane 6) for agarose gel electrophoresis. Similarly, the brightness of the ASODNs in the supernatants was observed from Lane 7 to Lane 10. And the related concentrations of the ASODNs are 3.29, 4.29, 5.29, and 6.29 μg/mL in the water phase during the synthetic process of the ASODNs-CPNPs. The detection limit concentration of ASODNs was estimated to be 0.60 μg/mL, and unloaded ASODNs were detected until the concentration of ASODNs in ASODNs-CPNPs was 5.29 μg/mL in aqueous solution of microemulsion mixture. Furthermore, based on the standard curve based method (Figure 3B), ASODNs loading efficiency of the nanoparticles was calculated to be more than 90%, indicating that CPNPs presented high loading capacity towards ASODNs.

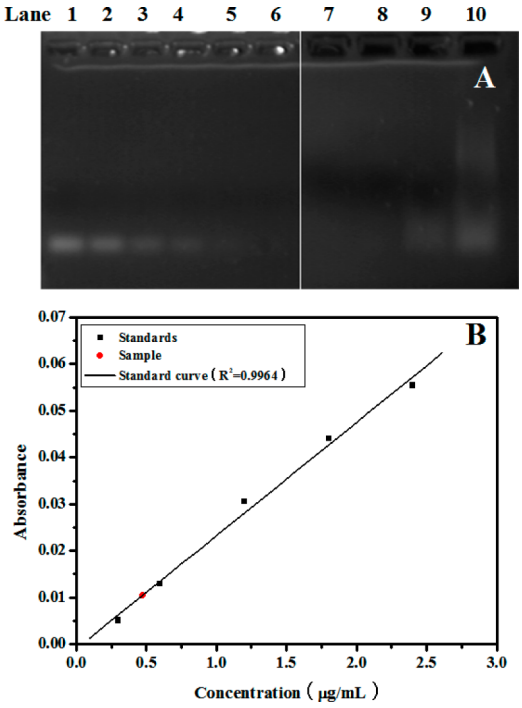

Figure 3. (A) Agarose gel electrophoresis of standard and unloaded ASODNs. Lanes from left to right: standard ASODNs (from Lane 1 to Lane 6) and different sample supernatants (from Lane 7 to Lane 10). (B) The supernatant of ASODNs-CPNPs (red) and the standard curve of ASODNs were recorded by multiskan spectrum at 260 nm for calculating the loading efficiency.

pH-Sensitive Release of ASODNs from ASODNs-CPNPs. As shown in Figure 4B, the dissolution of ASODNs-CPNPs increased rapidly initially and then gradually reached plateau for next 48 h at the same pH values. Meanwhile, the dissolution of ASODNs-CPNPs gradually increased with the decreasing pH from 7.00 to 4.00 (Figure 4A). These results suggested that the release of ASODNs from the nanoparticles was related with pH and time, respectively. It is well known that tumor tissues or cancer have a more acidic microenvironment, because of the production of lactic acid in acidic and hypoxia intracellular organelles.[34,35] Therefore, this drug carrier system had potential clinical applications for cancer therapy through controlled release of ASODs with stimulation of acidic microenvironment of cancer cells.

Cellular Transfection Analysis. The confocal laser microscopy and flow cytometry were used in the qualitative and quantitative assay for the transfection of HeLa cells with ASODNs-CPNPs. FAM was introduced onto the ASODs-CPNPs as fluorescence labeling agent. HeLa cells were incubated with 6′-FAM-ASODNs-CPNPs for 4 h, and then analyzed to evaluate the delivery ability of the nanoparticles. The confocal laser scanning microscopy studies reveal that a large amount of 6′-FAM-ASODNs-CPNPs successfully entered into the HeLa cells after 4 h incubation (Figure 5A). Moreover, flow cytometry analysis showed that the transfection efficiency was 98.45% (Figure 5B). All of these results demonstrated that the ASODNs-CPNPs can transport DNA into the cells effectively, and might be utilized as an efficient gene delivery vector.

Cellular Uptake Investigation of the ASODNs-CPNPs. We further determined the subcellular distribution of the ASODNs-CPNPs after its uptake into cell. As shown in Figure 6A, ASODNs-CPNPs could be detected in the HeLa cell by biological TEM. The nanoparticles were observed in cytoplasm and transported into nucleus within 4 h of incubation. Moreover, confocal images of cells after incubation with 6′-FAM-ASODNs-CPNPs for 4 h showed that the nanoparticles were mainly localized in the cell nucleus and just a few were

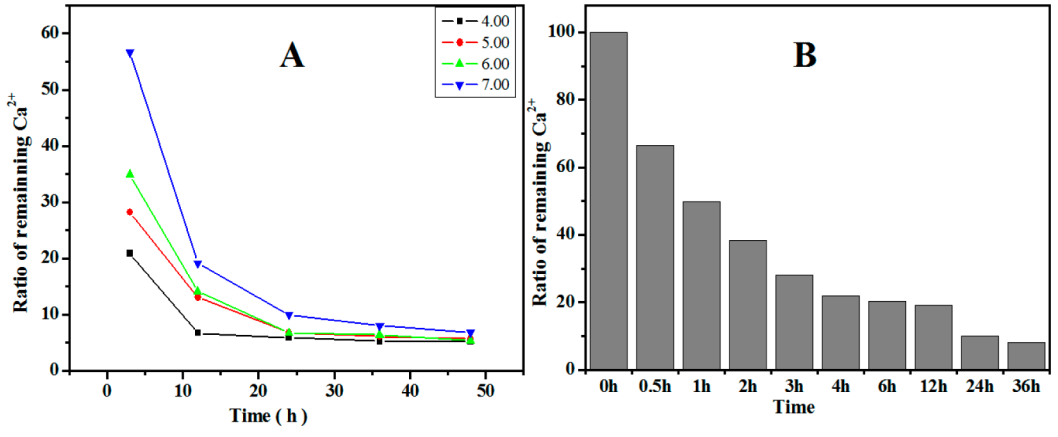

Figure 4. (A) pH values responding of ASODNs-CPNPs; (B) stained release responding of ASODNs-CPNPs.

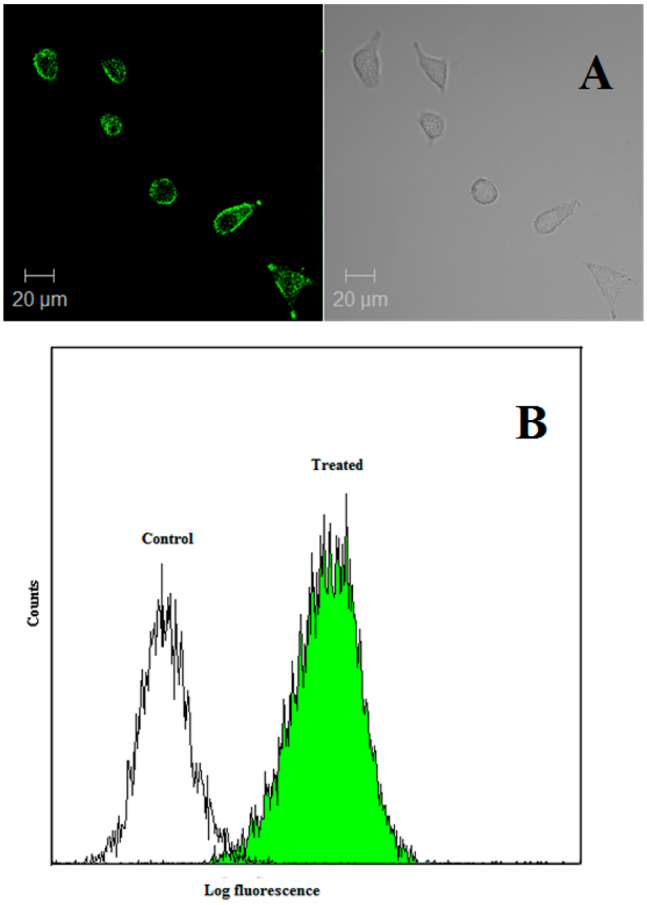

Figure 5. Cellular uptake of 6′-FAM-ASODNs-CPNPs. (A) Confocal laser scanning microscopy was used to follow intracellular distribution patterns of 6′-FAM -ASODNs-CPNPs for 4 h in HeLa cells. (B) Flow cytometry analysis comparing 6′-FAM-ASODNs-CPNPs treated cells for 4 h to untreated controls.

observed in the cytoplasm. (Figure 6B). This result was further verified by localization of 6′-FAM-ASODNs-CPNPs (green) with a commercially available nucleic marker propidium iodide (red) in cells at 37 °C. As shown in Figure 6C, the area of orange-yellow staining was the overlay of 6′-FAM-ASODNs-CPNPs (green) with propidium iodide (red). The results suggested that the nanoparticles had been transported into cell nucleus successfully.

Cell Viability Assay. Finally, cytotoxicity of ASODNs-CPNPs was assessed by its incubation of cells for 24 h, 48 h and 72 h. As shown in Figure 7, above 50% of cell growth inhibition

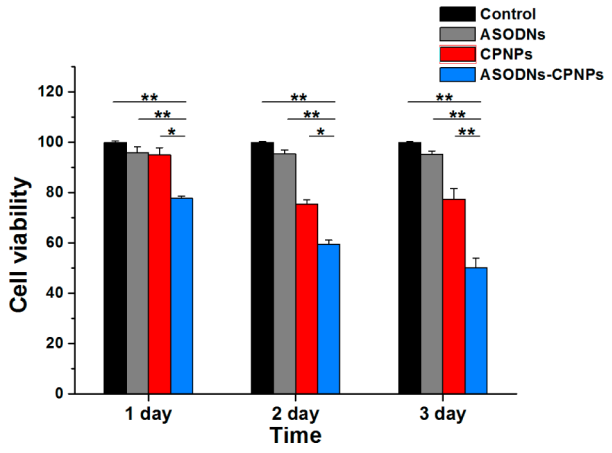

Figure 7. Cell viability was studied with the MTT assay at different time points (24, 48, and 72 h) after treatment with the ASODNs-CPNPs and other relative control compounds. *P < 0.05 and **P < 0.01, all bars show mean ± S.D., the data were taken from quarter independent experiments.

was achieved with ASODNs-CPNPs concentrations of 14.4 μg/mL after its incubation with HeLa cells for 72 h. In contrast, 94 and 72% of viable cells were detected after the cells treated with the same concentration of pure ASODNs and CPNPs, respectively. It indicated that the CPNPs based ASODNs carrier system could enhance the bioavailability of ASODNs, whereas the carrier itself exhibited nonspecific cytotoxicity under the same incubation conditions. Furthermore, results of cell viability at different time intervals exhibited that the inhibitory effect of nanoparticles on cells gradually increased with time. This because the increasing amounts of ASODNs-CPNPs had entered into the cells and released ASODNs with time. Therefore, the CPNPs-based biocarriers showed a great potential in delivering oligodeoxynucleotides for cancer therapy.

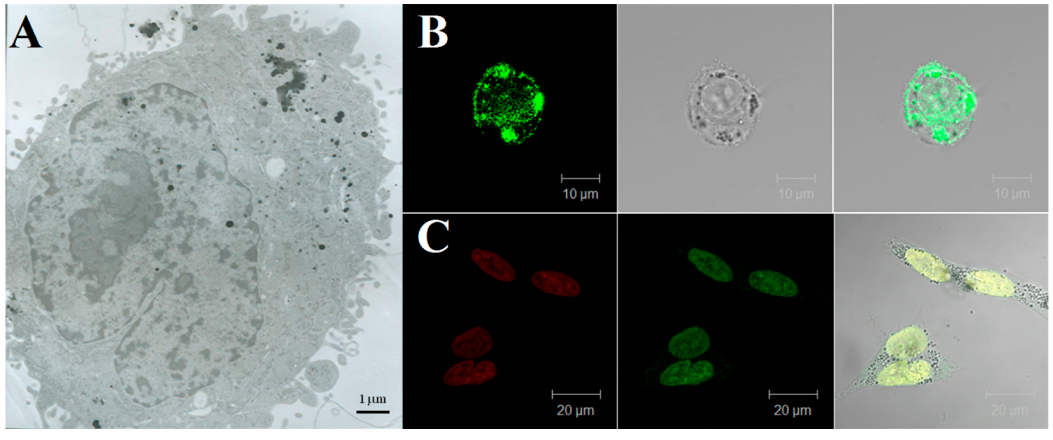

Figure 6. Internalization of ASODNs-CPNPs by HeLa cells. (A) Biological TEM micrograph of HeLa cell incubated with nanocomposites for 4h; (B) intracellular distribution patterns of 6′-FAM-ASODNs-CPNPs (green) in HeLa cells; (C) colocalization of 6′-FAM-ASODNs-CPNPs (green) and PI (red) implied nuclear localization.

dx.doi.org/10.1021/am3028926 | ACS Appl. Mater. Interfaces 2013, 5, 1131−1136

CONCLUSION

In summary, we have prepared the void spherical ASODNs-CPNPs using a facile microemulsion method. The structure morphology and composition of the nanocomposites was studied. The drug delivery capability of ASODNs-CPNPs was further explored and extracellular drug release was achieved. Cell imaging experiments and flow cytometry analysis demonstrated that the nanoparticles could be easily endocytosed into cells. MTT assay indicated that relatively lower cytotoxicity of CPNPs was observed even 3 days later, which suggested the biocompatibility of this CPNPs-based vector. Furthermore, the growth inhibition of ASODNs-CPNPs treated cells was obviously higher than the pure ASODNs treated ones in the same conditions. Such drug carriers system can be applied to help protect ASODNs from the degradation by enzymes (nucleases) existing in the cytoplasm. Overall, the synthesized ASODNs-CPNPs with their biocompatibility and biodegradability offer a potential application in delivering ASODNs for cancer therapy.

AUTHOR INFORMATION

Corresponding Author

*Tel.: +86 21 64321045. Fax: +86 21 64321833. E-mail: nqjia@shnu.edu.cn.

Author Contributions

†These authors contributed equally.

Notes

The authors declare no competing financial interest.

ACKNOWLEDGMENTS

This work was supported by Program for Shanghai Sci. & Tech. and Education Committee (12JC1407200, 09SG43), National 973 Project (2010-CB933901), New Century Excellent Talents in University (NCET-08-0897), Shanghai Key Laboratory of Rare Earth Functional Materials, Shanghai Normal University.

REFERENCES

(1) Rodríguez, J. A.; Span, S. W.; Ferreira, C. G.; Kruyt, F. A.; Giaccone, G. *Exp. Cell Res.* **2002**, *275*, 44−53.
(2) Shin, S.; Sung, B. J.; Cho, Y. S.; Kim, H. J.; Ha, N. C.; Hwang, J. I.; Chung, C. W.; Jung, Y. K.; Oh, B. H. *Biochemistry* **2001**, *40*, 1117−1123.
(3) Mahotka, C.; Wenzel, M.; Springer, E.; Helmut, E.; Gabbert, H. E.; Gerharz, C. D. *Cancer Res.* **1999**, *59*, 6097−6102.
(4) Prigodich, A.E.; Seferos, D.S.; Massich, M.D.; Giljohann, D.A.; Lane, B.C.; Mirkin, C.A. *ACS NANO.* **2009**, *3*, 2147−2152.
(5) Li, S.D.; Huang, L. *Mol. Pharm.s* **2006**, *3*, 579−588.
(6) Peng, J. F.; He, X. X.; Wang, K. M.; Tan, W. H.; Li, H M..; Xing, X. L.; Wang, Y. *Nanotechnology: N.B.M.* **2006**, *2*, 113−20.
(7) Martimprey, H. de; Vauthier, C.; Malvy, C.; Couvreur, P. *Eur. J. Pharm. Biopharm.* **2009**, *71*, 490−504.
(8) Wang, Y.; Nakamura, K.; Liu, X. R.; Kitamura, N.; Kubo, A.; Hnatowich, D. J. *Bioconjugate Chem.* **2007**, *18*, 1338−43.
(9) Keefe, A. D.; Pai, S.; Ellington, A. *Nat. Rev. Drug Discovery* **2010**, *9*, 537−550.
(10) Weyermann, J.; Lochmann, D.; Zimmer, A. *J. Controlled Release* **2004**, *100*, 411−423.
(11) Xu, Z.P.; Zeng, Q. H.; Lu, G. Q.; Yu, A. B. *Chem. Eng. Sci.* **2006**, *61*, 1027−4100.
(12) Faria, M.; Spiller, D.G.; Dubertret, C.; Nelson, J. S.; Mike, R. H.; Scherman, D. *Nat. Biotechnol.* **2001**, *19*, 40−44.
(13) Jeong, J.H.; Kim, S.W.; Par,k, T.G. *Bioconjugate Chem.* **2003**, *14*, 473−479.
(14) Wang, Y.; Nakamura, K.; Liu, X. R.; Kitamura, N.; Kubo, A.; Hnatowich, D. J. *Bioconjugate Chem.* **2007**, *18*, 1338−1343.
(15) Bhakta, G.; Mitra, S.; Maitra, A. *Biomaterials* **2005**, *26*, 2157−2163.
(16) Liu, J. Y.; Huang, W.; Pang, Y.; Zhu, X. Y.; Zhou, Y. F.; Yan, D. Y. *Biomaterials* **2010**, *31*, 5643−5651.
(17) Ding, X. R.; Wang, F.; Duan, M.; Yang, J.; Wang, S. Q. *Arch. Virol.* **2009**, *154*, 9−17.
(18) Park, J .S.; Na, K.; Woo, D. G.; Yang, H. N.; Kim, J. *Biomaterials* **2010**, *31*, 124−132.
(19) Giljohann, D. A.; Seferos, D. S.; Prigodich, A. E.; Pate,l, P. C.; Mirkin, C. A. *J. Am. Chem. Soc.* **2009**, *131*, 2072−2073.
(20) Bhakta, G.; Mitra, S.; Maitra, A. *Biomaterials* **2005**, *26*, 2157−2163.
(21) Gu, Z.; Rolfe, B. E.; Xu, Z. P.; Thomas, A. C.; Campbell, J. H.; Lu, G. Q. *Biomaterials* **2010**, *31*, 5455−5462.
(22) Miyata, K.; Gouda, N.; Takemoto, H.; Oba, M.; Lee, Y.; Koyama, H. *Biomaterials* **2010**, *31*, 4764−4770.
(23) Sokolova, V.; Kovtun, A.; Heumann, R.; Epple, M. *J. Biol. Inorg. Chem.* **2007**, *12*, 174−179.
(24) Singh, R.; Saxena, A.; Mozumdar, M. *Int. J. Appl. Ceram. Tec.* **2008**, *5*, 1−10.
(25) Chen, Y.; Deng, L.B.; Maeno-Hikichi, Y.; Lai, M. Z.; Chang, S. H.; Chen, G. *Cell* **2003**, *115*, 37−48.
(26) Cai, Y. R.; Liu, Y. K.; Yan, W. Q.; Hu, Q. H.; Tao, J. H.; Zhang, M. *J. Mater. Chem.* **2007**, *17*, 3780−3787.
(27) Sokolova, V.; Radtke, I.; Heumann, R.; Epple, M. *Biomaterials* **2006**, *27*, 3147−3153.
(28) Chen, F.; Huan,g, P.; Zhu, Y. J.; Wu, J.; Cui, D. X. *Biomaterials* **2012**, *33*, 6447−6455.
(29) Wu, G. J.; Zhou, L. Z.; Wang, K. W.; Chen, F.; Sun, Y.; Duan, Y.,R.; Zhu, Y. J.; Gu, H. C. *J. Colloid Interface Sci.* **2010**, *345*, 427−432.
(30) Olton, D.; Li, J. H.; Wilson, M. E.; Rogers, T.; John, C.; Huang, L. *Biomaterials* **2007**, *28*, 1267−1279.
(31) Isobe, T.; Nakamura, S.; Nemoto, R.; Senna, M. S. *Phys. Chem. B* **2002**, *106*, 5169−5176.
(32) Singh, S.; Bhardwaj, P.; Singh, V.; Aggarwal, S.; Mandal, U. K. *J. Colloid Interf. Sci.* **2008**, *319*, 322−329.
(33) Morgan, T. T.; Muddana, H. S.; Altinoğlu, E. I.; Rouse, S. M.; Tabaković, A.; Tabouillot, T. *Nano.Lett.* **2008**, *8*, 4108−4115.
(34) Chowdhury, E.H.; Maruyama, A.; Kano, A.; Nagaoka, M.; Kotaka, M.; Hirose, S. *Gene.* **2006**, *376*, 87−94.
(35) Wu, X. L.; Kim, J. H.; Koo, H.; Bae, S. M.; Shin, H.; Kim, M. S. *Bioconjugate Chem.* **2010**, *21*, 208−213.